The road to residency

Uncovering the proteome, metabolism and transcriptional networks of tissue-resident memory T cells

Beumer-Chuwonpad, A.

Publication date
2023

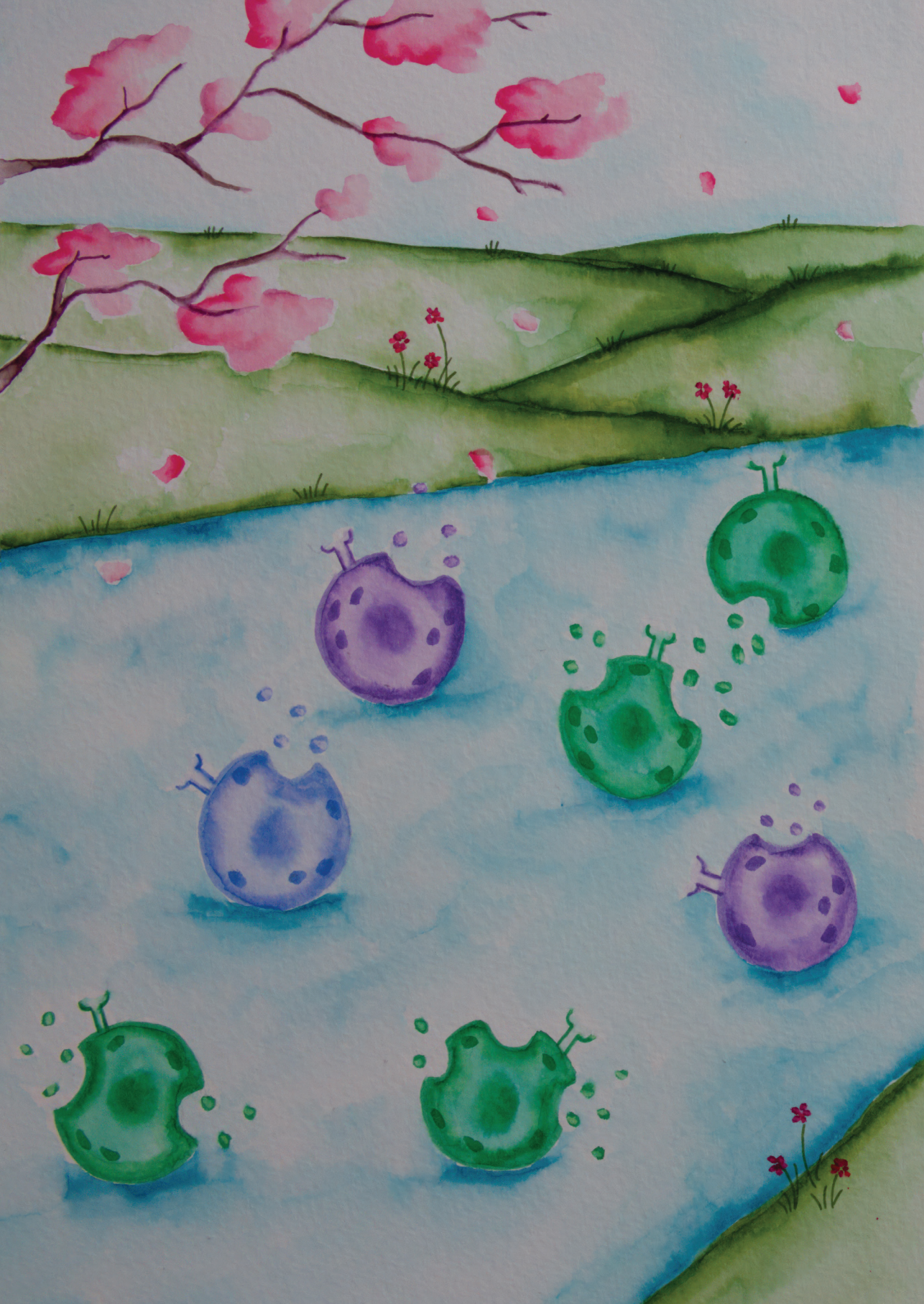

CHAPTER 6

Hobit and Blimp-1 regulate T_{RM} abundance after *LCMV* infection by suppressing tissue exit pathways of T_{RM} precursors

Loreto Parga-Vidal[1], Renske L.R.E. Taggenbrock[1]*, Ammarina Beumer-Chuwonpad[1]*, Hajar Aglmous[1], Natasja A.M. Kragten[1], Felix M. Behr[1,2], Astrid A. Bovens[1], René A.W. van Lier[1], Regina Stark[1,2,3], and Klaas P.J.M. van Gisbergen[1,2]

[1] Department of Hematopoiesis, Sanquin Research and Landsteiner Laboratory, Amsterdam UMC, University of Amsterdam, the Netherlands

[2] Department of Experimental Immunology, Amsterdam UMC, University of Amsterdam, The Netherlands

[3] BIH Center for Regenerative Therapies, Charité Universitätsmedizin Berlin, Germany

* These authors contributed equally

European journal of immunology (2022) 52(7):1095-1111

Abstract

Upon resolution of acute viral infections, a minor population of effector $CD8^+$ T cells persists as memory precursor effector T cells (MPECs). These effector T cells have the capacity to form memory $CD8^+$ T cells that are retained as tissue-resident memory T cells (T_{RM}) in peripheral tissues. We have previously shown that the transcription factor Hobit and its homolog Blimp1 drive T_{RM} development in several tissues after viral infection, but how and when these transcription factors mediate T_{RM} formation remains poorly understood. In particular, the major impact of Blimp-1 in regulating several aspects of effector T cell differentiation impairs study of the specific role of this transcription factor in T_{RM} development. Here, we used the restricted expression of Hobit in the T_{RM} lineage to develop mice with a conditional deletion of Blimp1 in T_{RM}, allowing us to investigate the role of both transcription factors in T_{RM} precursors without affecting the early, Blimp1 dependent steps, in effector T cell differentiation. We found that both Hobit and Blimp1 were required for the upregulation of CD69 on virus-specific T_{RM} precursors after *LCMV* infection, underlining a role of these transcription factors in the retention of T_{RM} precursors within tissues. The early impact of Hobit and Blimp1 favored T_{RM} formation and prevented the development of circulating memory T cells. Thus, our findings highlight a role of Hobit and Blimp1 at the branching point of circulating and resident memory lineages by suppressing tissue egress of T_{RM} precursors at early stages of infection.

Introduction

Immunity against intracellular pathogens relies on $CD8^+$ T cells that can specifically eliminate infected cells through the production of cytotoxic molecules and pro-inflammatory cytokines. $CD8^+$ T cell responses start with the priming of naïve $CD8^+$ T cells by recognition of pathogen-derived antigens presented on antigen-presenting cells (APCs) in the lymph nodes (LNs). Antigen-triggered $CD8^+$ T cells proliferate and differentiate into effector T cells that migrate to the site of infection, where they eradicate the pathogen[1,2]. The majority of effector $CD8^+$ T cells undergo a program of terminal differentiation and perish once the pathogen is cleared. These terminal effector cells are known as short-lived effector cells (SLECs). A minor effector population, termed memory precursors effector cells (MPECs), survives and retains the capacity to develop into memory $CD8^+$ T cells[3,4]. Differences in the migration pattern and function classify memory $CD8^+$ T cells into circulating and resident memory T cells. Circulating memory T cells consist of central memory (T_{CM}) and effector memory $CD8^+$ T cells (T_{EM}), that continuously patrol the body in search of invading pathogen[5]. In contrast, tissue-resident memory $CD8^+$ T cells (T_{RM}) permanently reside in peripheral tissues and provide enhanced local protection against reinfection, given their strategic location at sites of pathogen entry and their ability to rapidly upregulate effector functions[6,7].

Several transcription factors have been implicated in driving antigen-triggered $CD8^+$ T cells towards either a terminal or a memory stage upon infection. The transcription factors Runx3, Blimp1, Tbet, Notch and Id2 have been described to mediate terminal effector $CD8^+$ T cell differentiation and the acquisition of effector functions[3,8–12]. In contrast, the transcription factors Eomes, Bcl6 and Id3 have been implicated in promoting memory T cell development[12–16]. Although several transcription factors have been shown to regulate the development of memory T cells, how and when antigen-triggered $CD8^+$ T cells branch into resident and circulating memory lineages remains poorly understood.

We have recently described that the T_{RM} lineage is already established during the effector stage of the immune response upon viral infection. We have characterized a subset of effector $CD8^+$ T cells in tissues as T_{RM} precursors, which are biased to form T_{RM} rather than circulating memory T cells[17]. These committed T_{RM} precursors were specifically identified by expression of the T_{RM}-restricted transcription factor Hobit[17]. Early commitment to the T_{RM} lineage was also observed by others. During priming, signals from type 1 classical dendritic cells in the draining LNs appear specifically required to favor the development of effector $CD8^+$ T cells into T_{RM} in the skin[18]. A recent study has shown that T cell clones with a higher propensity to form T_{RM} are present in the circulation before tissue entrance after skin vaccination[19]. Furthermore, the transcription factor Id3 identifies effector $CD8^+$ T cell with elevated potential to form T_{RM} in the small intestine[20,21]. Altogether, these findings underline that the transcriptional program driving the separation of the T_{RM} lineage from circulating memory T cells and terminal effector T cells takes place at early stages of the immune response.

Previously, we have demonstrated that Hobit and its homolog Blimp1 are essential for the formation of $CD8^+$ T_{RM} cells throughout tissues, including skin, liver, kidneys, and the small intestine[22]. However, how and when Hobit and Blimp1 instruct the branching off of T_{RM} from terminal effectors and circulating memory T cells upon infection remains unresolved. Expression of Hobit appears highly restricted to the T_{RM} lineage and allows for the unequivocal identification of T_{RM} precursors[17,22]. In contrast, Blimp1 is broadly expressed in antigen-experienced T cells and promotes terminal differentiation of effector $CD8^+$ T cells besides instructing T_{RM} formation[8,9,22]. Given that Blimp1 has a major impact in multiple processes involving effector $CD8^+$ T cell differentiation, it has not yet been possible to investigate the specific role of Blimp1 in the T_{RM} lineage. Therefore, exploiting the specific expression pattern of Hobit, we developed mice with a conditional deletion of Blimp1 within the T_{RM} lineage to specifically investigate the role of both Hobit and Blimp1 in T_{RM} differentiation. In the absence of Hobit, T_{RM}-specific deletion of Blimp1 reduced T_{RM} formation. Interestingly, T_{RM} precursors formed in the absence of Hobit and Blimp1, but displayed impaired upregulation of CD69 expression, indicating a dedicated role of both transcription factors in the early suppression of tissue egress. Thus, our results show that Hobit and Blimp1 cooperatively contribute to the upregulation of CD69 in T_{RM} precursors during the effector phase of the immune response, which favors the subsequent formation of T_{RM} cells.

Results

Hobit expression is restricted to the T_{RM} lineage and Blimp1 is widely expressed in antigen-experienced CD8$^+$ T cells.

To evaluate the expression of Hobit and Blimp1 in virus-specific CD8$^+$ T cells at different stages of the immune response, we infected Hobit$^{tdTom/WT}$ Blimp$^{GFP/WT}$ (HR BI^{GFP}) mice, that simultaneously report Hobit and Blimp1 expression, with *lymphocytic choriomeningitis virus* (*LCMV*) Armstrong. The differentiation of virus-specific (Db Gp33$^+$) CD8$^+$ T cells into memory CD8$^+$ T cells was monitored in spleen, liver, kidney and intra-epithelial lymphocytes (IEL) of the small intestine (SI) at >30 days post-infection (p.i.). Virus-specific CD8$^+$ memory T-cells were classified based on the expression of CD62L and CD69 into T_{CM} (CD62L$^+$ CD69$^-$), T_{EM} (CD62L$^-$ CD69$^-$) and T_{RM} (CD62L$^-$ CD69$^+$) (figure S1A). In line with our previous studies23, we found that Hobit (tdTomato) expression was confined to the T_{RM} compartment (figure 1A-B). In contrast, Blimp1 (GFP) was widely expressed in T_{CM}, T_{EM} and T_{RM}, although Blimp1 expression was lower in T_{CM} compared to the other memory fractions (figure 1C-E), as previously reported[9,24]. Accordingly, transcriptional analysis showed that Blimp1 expression was increased in all memory CD8$^+$ T cell subsets in comparison to the naïve compartment (figure S1B). These data underline that Hobit expression is restricted to T_{RM} while Blimp1 is broadly expressed in circulating and resident CD8$^+$ T cells during the memory phase of infection.

We have recently found that Hobit identifies effector CD8$^+$ T cells that have committed to the T_{RM} lineage[17]. Previous studies have shown that Blimp1 upregulation also takes place during the effector phase after viral infection, but the expression of Blimp1 in T_{RM} precursors has remained unknown. Analysis of *LCMV*-specific CD8$^+$ T cells at day 8 p.i. showed higher expression of Blimp1 in (CD127$^-$KLRG1$^+$) SLECs compared to (CD127$^+$KLRG1$^-$) MPECs (figure S1C-E), as previously reported[8,9]. We found that Hobit$^+$ virus-specific effector CD8$^+$ T cells consistently expressed slightly lower levels of Blimp1 compared to Hobit$^-$ cells in the spleen, liver and kidney, but not in the SI IEL (figures 1F-G and S1F). Transcriptional analysis showed that Blimp1 is upregulated in total effector CD8$^+$ T cells compared to naïve CD8$^+$ T cells, but did not reveal significant differences between Hobit$^-$ and Hobit$^+$ subsets of effector CD8$^+$ T cells (figure S1G). Thus, these results show that Hobit expression is confined to the T_{RM} lineage, whereas Blimp-1 is broadly upregulated in effector CD8$^+$ T cells including T_{RM} precursors and maintained in all subsets of memory CD8$^+$ T cells after viral clearance.

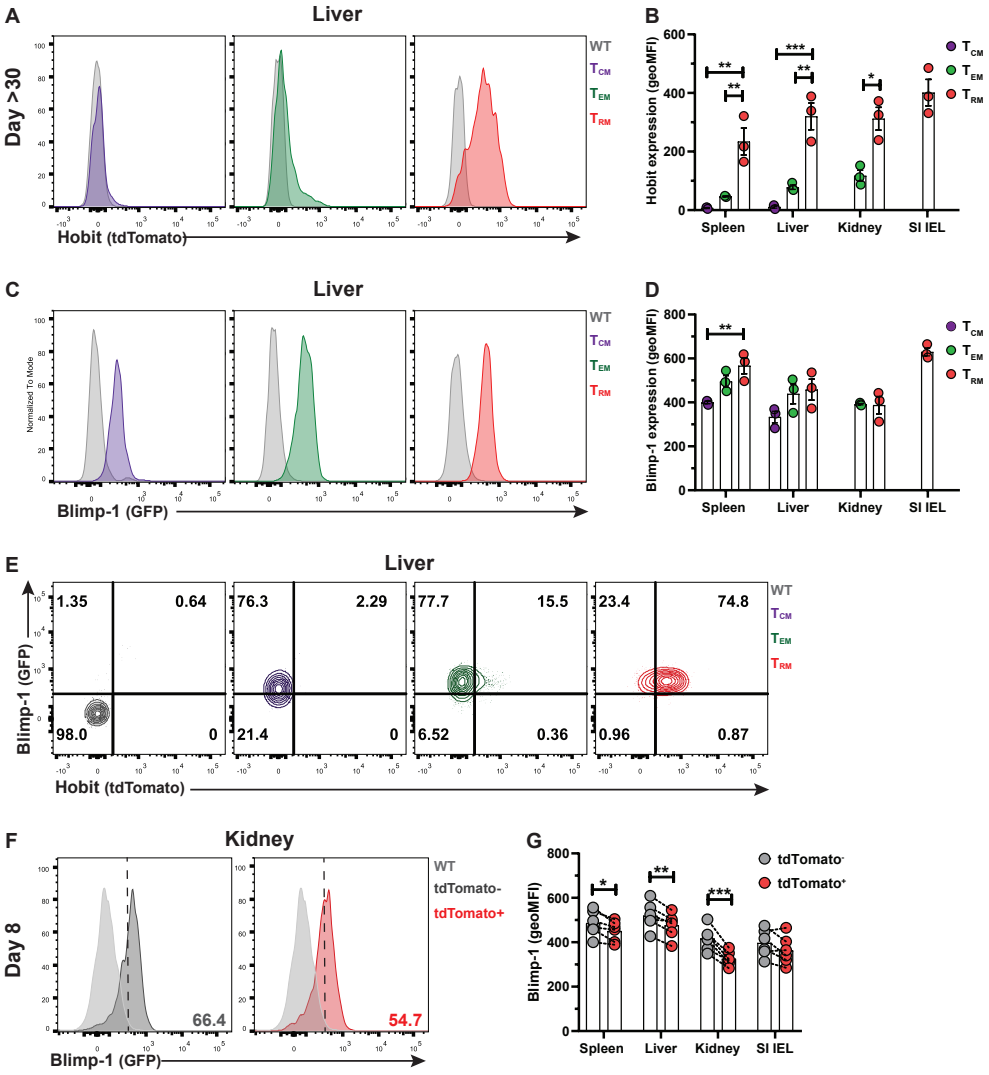

Figure 1. Hobit is restricted to the T_{RM} lineage and Blimp1 is widely expressed in antigen-experienced $CD8^+$ T cells. Wild type control (WT) and HR BI^{GFP} mice were infected with *LCMV* Armstrong and virus-specific ($Gp33^+$) $CD8^+$ T cells were analyzed by flow cytometry at day 8 and day >30 post-infection (p.i.). (A-D) Representative histograms depict (A) tdTomato (Hobit) and (C) GFP (Blimp1) expression in $Gp33^+$ T_{CM}, T_{EM} and T_{RM} from WT (grey) and HR BI^{GFP} mice at day >30 p.i. (B, D) The geometric mean fluorescence intensity (geo MFI) of (B) tdTomato and (D) GFP expression was quantified in $Gp33^+$ $CD8^+$ T cells from the indicated tissues. (E) Representative flow cytometry plots display expression of GFP and tdTomato in virus-specific memory $CD8^+$ T cells from the liver. (F) Representative histograms depict GFP expression in WT and $tdTomato^+$ and $tdTomato^-$ $Gp33^+$ $CD8^+$ T cells of HR BI^{GFP} mice at day 8 p.i. (G) The geo MFI of GFP expression was quantified in $tdTomato^+$ and $tdTomato^-$ cells in the indicated tissues. (H) Representative flow cytometry plots display expression of GFP and tdTomato in virus-specific $CD8^+$ T cells from the kidney of WT and HR BI^{GFP} mice at day 8 p.i. (A-H) Symbols represent individual mice. Error bars represent mean ± SEM. (A-E) Representative data of one ($n = 4$) out of two independent experiments. Bars represent the mean. One-way ANOVA; (F-H) Combined data from two independent experiments ($n = 6$). Dotted lines connect paired samples. Paired *t*-test; * $P < 0.05$; ** $P < 0.01$; *** $P < 0.001$.

Hobit and Blimp1 instruct the separation between the T_{RM} and T_{CM} lineages upon Hobit upregulation.

We have previously addressed the role of Hobit and Blimp1 in memory CD8$^+$ T cell differentiation using mice that completely lacked Hobit and Blimp1 in the T cell lineage[22]. These Hobit and Blimp1 double deficient mice have defects in both terminal effector and T_{RM} differentiation, complicating the study of the specific role of these transcription factors in the T_{RM} lineage. Here, we have used the newly developed reporter Hobit$^{tdTom/KO}$ Blimp$^{fl/fl}$ (HR^{KO} Bl^{fl}) mice to specifically address the role of Hobit and Blimp1 within the T_{RM} lineage (figure S2A). One of the Hobit alleles of the HR^{KO} Bl^{fl} mice is disrupted by a trapping cassette while the other allele is disrupted by insertion of the Hobit reporter construct, resulting in functional deficiency of Hobit, but permitting tracking of the transcriptional activity at the Hobit locus through tdTomato expression (figure S2A). The Hobit driven Cre-recombinase is designed to mediate the excision of the floxed Blimp1 allele in Hobit$^+$expressing cells (figure S2A). Given that Hobit is only consistently expressed in T_{RM} precursors at day 8 after infection[17], these mice offer a unique opportunity to address the role of Blimp1 in the T_{RM} lineage without affecting early effector CD8$^+$ T cell differentiation. To assess the efficiency of the Hobit$^+$driven Cre-recombinase to delete Blimp1 in T_{RM}, tdTomato$^+$ and tdTomato$^-$ memory CD8$^+$ T cells were isolated from the liver and SI IEL of *LCMV*-infected HR^{KO} Bl^{fl} and control HR mice at day >30 p.i. Using PCRs that distinguish the deleted from the non-deleted Blimp1 locus, we observed that the Blimp1 gene was largely deleted in tdTomato$^+$ CD8$^+$ T cells from both liver and SI IEL of HR^{KO} Bl^{fl} mice, but not in tdTomato$^-$ CD8$^+$ T cells of these mice or in CD8$^+$ T cells from these organs of control HR mice (figure S2B). Conversely, the non-deleted Blimp1 gene was detected more strongly in the tdTomato$^-$ fraction compared to the tdTomato$^+$ fraction of CD8$^+$ T cells of HR^{KO} Bl^{fl} mice (figure S2C). Thus, the HR^{KO} Bl^{fl} mouse enabled us to specifically address the role of Hobit and Blimp1 during T_{RM} development.

We followed the differentiation of virus-specific (Gp33$^+$) memory CD8$^+$ T cells in *LCMV*-infected HR^{KO} Bl^{fl} and control HR mice. The formation of Gp33$^+$ memory T cells was comparable between HR^{KO} Bl^{fl} and HR mice in blood, peripheral lymph nodes (pLN), and peripheral tissues including liver, kidney and IEL and lamina propria (LPL) of the small intestine at day >30 p.i (figure 2A-B). An increase in the percentage of Gp33$^+$ memory CD8$^+$ T cells was observed in spleen of HR^{KO} Bl^{fl} mice compared to HR mice (figure 2B). Analysis of memory CD8$^+$ T cell subsets showed reduced formation of tdTomato$^+$ T_{RM} in spleen, liver and kidney (figure 2C-D), but not in the IEL and LPL compartment of the small intestine of HR^{KO} Bl^{fl} mice compared to HR mice (figure 2C-D). In contrast, we observed increased formation of T_{CM} in spleen and pLN of HR^{KO} Bl^{fl} mice compared to HR mice (figure 2E and F). These findings suggest that Blimp1 acts within the T_{RM} lineage after upregulation of Hobit to instruct T_{RM} formation together with Hobit. Moreover, our data indicate that Hobit and Blimp1 impair the development of T_{CM}.

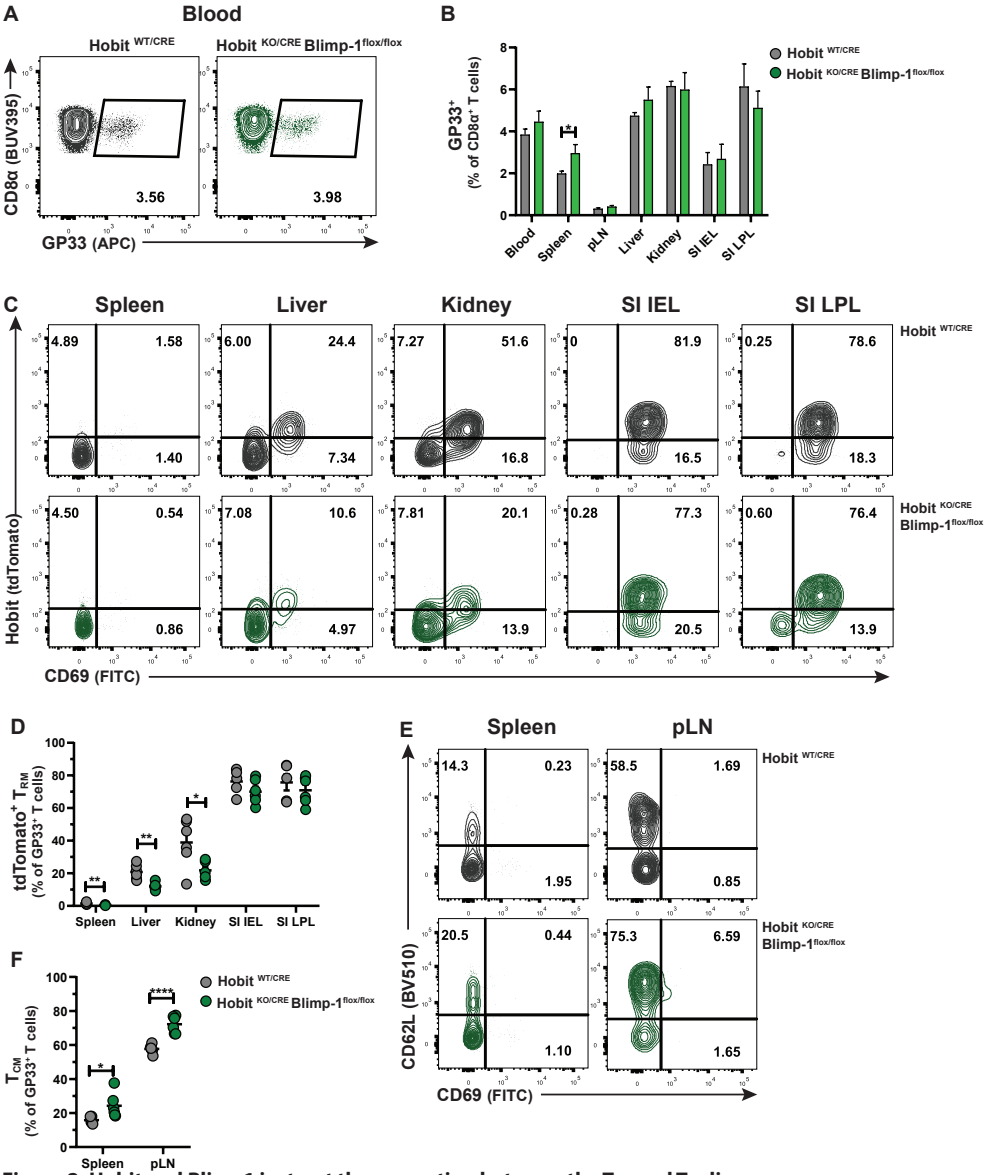

Figure 2. Hobit and Blimp1 instruct the separation between the T_{RM} and T_{CM} lineages.
HR and HR^{KO} BI^{fl} mice were infected with *LCMV* Armstrong and virus-specific ($Gp33^+$) $CD8^+$ T cells were analyzed by flow cytometry at day >30 post-infection (p.i.). (A) Flow cytometry plot displays the binding of Db Gp33 tetramers to $CD8^+$ T cells from the blood of HR and HR^{KO} BI^{fl} mice. (B) The frequency of the *LCMV*-specific $CD8^+$ T cells was quantified. (C-F) Representative flow cytometry plots show (C) tdTomato and CD69 and (E) CD62L and CD69 expression in $Gp33^+$ $CD8^+$ T cells within the indicated tissues. The frequency of (D) $tdTomato^+$ T_{RM} and (F) T_{CM} within $Gp33^+$ $CD8^+$ T cells was quantified. Combined data from two independent experiments (n = 5-6). Symbols represent individual mice. Error bars represent mean ± SEM. Unpaired t-test; * $P < 0.05$; ** $P < 0.01$; **** $P < 0.0001$.

To exclude the potential impact of viral clearance on memory $CD8^+$ T cell differentiation, we generated mixed bone marrow (BM) chimeras with either WT and HR compartments or

WT and HR^{KO} BI^{fl} compartments in a 1:1 ratio (figures 3A and S3A). The HR and HR^{KO} BI^{fl} donor stem cells contributed equally compared to the WT donor stem cells to the establishment of $CD8^+$ T cells (figure S3B and C). WT-HR and WT- HR^{KO} BI^{fl} mixed BM chimeras were infected with *LCMV* Armstrong to analyze the virus-specific memory $CD8^+$ T cell response at day >30 after infection (figure 3A). The WT and HR compartments contributed similarly to the formation of $Gp33^+$ $CD8^+$ memory T cells in lymphoid and peripheral tissues of WT-HR BM chimeras (figure 3B and C). In contrast, the HR^{KO} BI^{fl} compartment was overrepresented in $Gp33^+$ memory $CD8^+$ T cells of lymphoid tissues, while this compartment was subtly underrepresented in virus-specific memory cells in peripheral tissues, including kidney and SI IEL of WT and HR^{KO} BI^{fl} mixed BM chimeras (figure 3B,D). Underlining the differences in the distribution of WT and HR^{KO} BI^{fl} memory $CD8^+$ T cells, we observed that T_{CM} in blood, spleen, pLN and mesenteric LNs (mesLN) were relatively increased within the HR^{KO} BI^{fl} compartment compared to the WT compartment (figure 3E-F), whereas T_{RM} in liver, kidney and SI IEL were substantially decreased in the HRKO BI^{fl} compartment relative to the WT compartment (figure 3E,G). In WT and HR mixed BM chimeras no differences were observed in the contribution of the donor compartments to the formation of T_{CM} and T_{RM} (figure 3E, H, I). Thus, these findings support that Hobit and Blimp1 instruct T_{RM} formation and restrict T_{CM} development in antigen-triggered $CD8^+$ T cells that have already passed the initial differentiation steps and have upregulated Hobit expression.

Blimp1 does not regulate terminal differentiation upon establishment of the T_{RM} lineage.

Recently, we have identified T_{RM} precursors through their specific expression of Hobit during the effector phase of infection[17]. To evaluate the impact of Hobit and Blimp1 on T_{RM} precursor formation, virus-specific effector $CD8^+$ T cells of *LCMV*-infected HR and HR^{KO} BI^{fl} mice were analyzed at day 8 p.i. We were able to identify tdTomato expression indicating upregulation of Hobit in a subset of effector $CD8^+$ T cells located in peripheral, but not in lymphoid tissues (figure 4A-B), in line with previous findings[17]. We did not observe differences in the presence of $tdTomato^+$ effector $CD8^+$ T cells between HR^{KO} BI^{fl} and control HR in blood, lymphoid tissues such as spleen and pLN, or in peripheral tissues including liver, kidney, SI IEL and SI LPLs (figure 4A- B), suggesting that lack of Hobit and Blimp1 does not compromise the presence of T_{RM} precursors within the tissues at day 8 post *LCMV* infection.

Previously, Blimp1 has been shown to induce terminal effector differentiation[8,9,25]. However, whether Blimp1 instructs terminal differentiation in already established T_{RM} precursors has not yet been addressed. We analyzed the distribution of ($KLRG1^-$ $CD127^+$) MPECs and ($KLRG1^+$ $CD127^-$) SLECs in the $tdTomato^+$ and $tdTomato^-$ fractions of both HR^{KO} BI^{fl} and control HR mice (figure 4C-H). We found no differences in KLRG1 and CD127 expression in circulation, lymphoid and peripheral tissues of HR^{KO} BI^{fl} and control HR mice, suggesting that Blimp1 does not affect terminal differentiation within the $Hobit^+$ lineage (figure 4C-H). Therefore, these results show that Blimp1 does not drive terminal differentiation upon establishment of T_{RM} precursors.

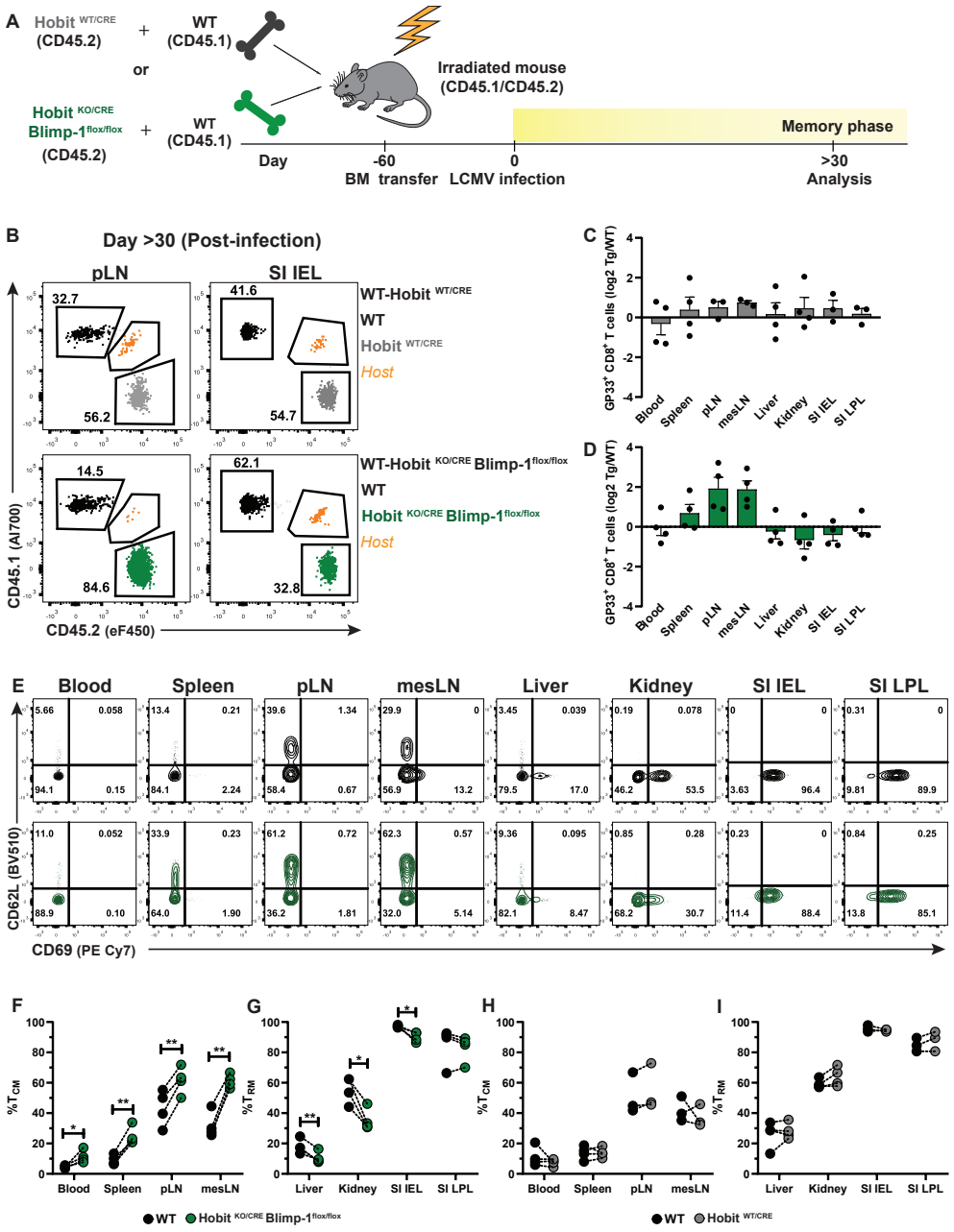

Figure 3. Hobit and Blimp-1 instruct T_{RM} fate after Hobit upregulation.
(A) Scheme shows the setup of the *LCMV* infection experiment in mixed bone marrow (BM) chimeras from WT and HR mice or WT and HR^{KO} BI^{fl} mice (1:1 ratio) to analyze virus-specific memory $CD8^+$ T cells at day >30 p.i. by flow cytometry. (B) Representative flow cytometry plots display CD45.1 and CD45.2 to identify the contribution of WT ($CD45.1^+$) and HR and HR^{KO} BI^{fl} ($CD45.2^+$) to the $Gp33^+$ $CD8^+$ T cell fraction in the indicated tissues at day >30 p.i. (C, D) The $\log_2$ ratio of $Gp33^+$ $CD8^+$ T cells of (C) HR (transgenic, tg) and (D) HR^{KO} BI^{fl} (tg) relative to WT controls was quantified in the indicated tissues. (E) Representative flow cytometry plots display expression of CD62L and

CD69 of *LCMV*-specific memory CD8$^+$ T cells of the WT (black) and HR^{KO} Bl^{fl} (green) compartment in the indicated tissues of WT-HR^{KO} Bl^{fl} chimeric mice. (F-I) The frequency of (F, H) T_{CM} and (G, I) T_{RM} within Gp33$^+$ CD8$^+$ T cells from WT and transgenic mice is displayed. Symbols represent individual mice. Dotted lines connect paired samples. Representative data of one (n = 3-4) out of two independent experiments. Paired t-test; * $P < 0.05$; ** $P < 0.01$.

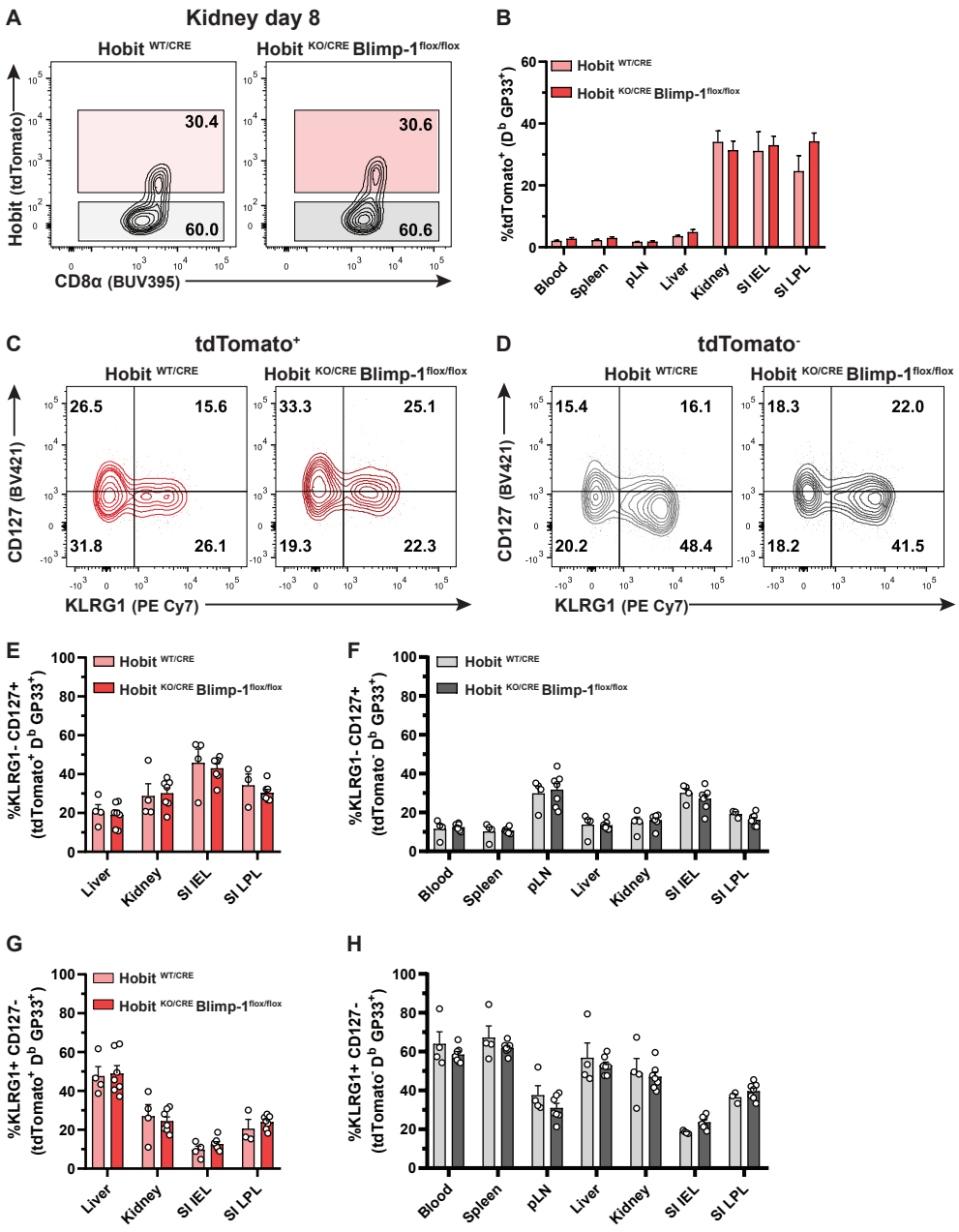

Figure 4. Blimp1 does not regulate terminal differentiation upon establishment of the T_{RM} lineage.
(A) Representative flow cytometry plots display tdTomato expression in Gp33$^+$ CD8$^+$ T cells isolated from the kidney of HR and HR^{KO} Bl^{fl} mice at day 8 after *LCMV* infection. (B) Expression of tdTomato was quantified in Gp33$^+$

CD8$^+$ T cells of HR and HR^{KO} Bl^{fl} mice in the indicated tissues at day 8 p.i. (C, D) Representative flow cytometry plots show expression of CD127 and KLRG1 within (C) tdTomato$^+$ or (D) tdTomato$^-$ virus-specific CD8$^+$ T cells isolated from the kidney of HR and HR^{KO} Bl^{fl} mice. (E-H) The percentage of (E, F) MPECs (KLRG1$^-$ CD127$^+$) and (G, H) SLECs (KLRG1$^+$ CD127$^-$) was determined within the (E, G) tdTomato$^+$ and (F, H) tdTomato$^-$ fraction of Gp33$^+$ CD8$^+$ T cells. Combined data from two independent experiments (n = 4-7). Symbols represent individual mice. Error bars represent mean ± SEM. Unpaired t-test.

Hobit and Blimp1 promote CD69 expression on T_{RM} precursors.

We next evaluated whether Hobit and Blimp1 affected the phenotype of T_{RM} precursors during the effector phase. For this purpose, we studied the expression of T_{RM}-associated molecules in tdTomato$^+$ and tdTomato$^-$ virus-specific effector CD8$^+$ T cells at day 8 p.i. Interestingly, we found a substantial reduction of CD69 expression in the tdTomato$^+$ fraction of liver, kidney, SI IEL and SI LPL of HR^{KO} Bl^{fl} compared to control HR mice (figure 5A-C). In contrast, the tdTomato$^-$ population remained largely unaffected (figure 5A, D-E). To determine whether Hobit, Blimp1 or both transcription factors were responsible for the downregulation of CD69 expression, we monitored the development of *LCMV*-specific effector CD8$^+$ T cells from single HR^{KO} and HR Bl^{fl} mice, in which either Hobit or Blimp-1 were specifically deleted from the T_{RM} lineage, respectively. Remarkably, we did not observe differences in CD69 expression in tdTomato$^+$ effector CD8$^+$ T cells in control HR, HR^{KO} or HR Bl^{fl} mice in contrast to the tdTomato$^+$ fraction of HR^{KO} Bl^{fl} mice, which showed a reduction in CD69 expression (figure S5A-D). These findings indicate that Hobit and Blimp1 cooperatively regulate CD69 expression. In contrast, no differences were observed in the expression of CD103 or the T_{RM}-associated molecules CD49a and CXCR617 on tdTomato$^+$ virus-specific effector CD8$^+$ T cells of control HR, HR^{KO}, HR Bl^{fl} or HR^{KO} Bl^{fl} mice (figure S5E-J), indicating that neither Hobit or Blimp1 drive the expression of CD103, CD49a and CXCR6 on T_{RM} precursors. Frequencies of CD62L$^+$ effector CD8$^+$ T cells in pLNs tended to be higher in HR^{KO} Bl^{fl} mice compared to HR mice (figure 5F and G), in line with the increased numbers of T_{CM} in the memory phase (figure 2 and 3). Altogether, these findings indicate that Hobit and Blimp1 cooperatively instruct upregulation of CD69 expression on Hobit$^+$ T_{RM} precursors.

Next, we developed mixed BM chimeras with control HR and HR^{KO} Bl^{fl} BM in a 1:1 ratio (figures 6A and S6A) to exclude impact of viral clearance on the Hobit and Blimp1-driven regulation of effector CD8$^+$ T cells. The donor HR and HR^{KO} Bl^{fl} stem cells contributed similarly to the establishment of the CD8$^+$ T cell lineage (figure S6B-C). Analysis of Gp33$^+$ T cells at day 8 after *LCMV* infection showed that the HR^{KO} Bl^{fl} compartment was at a disadvantage in populating peripheral organs such as kidney and small intestine compared to the HR compartment (figure 6B-C). The expression of tdTomato was equal in both HR and HR^{KO} Bl^{fl} virus-specific effector CD8$^+$ T cells (figure 6D). In line with our previous observations, tdTomato$^+$ effector CD8$^+$ T cells, but not tdTomato$^-$ effector CD8$^+$ T cells, from the HR^{KO} Bl^{fl} compartment displayed a reduction of CD69 expression compared to the HR compartment (figure 6E-G). Moreover, CD62L expression appeared slightly increased on the HR^{KO} Bl^{fl} fraction compared to the HR fraction of effector CD8$^+$ T cells in the pLNs (figure S6D-E). Taken together, these studies indicate that Hobit and Blimp1 instruct CD69 expression on effector CD8$^+$ T cells favoring the subsequent development of T_{RM} during the memory phase of the immune response. Thus, Hobit and Blimp1-driven CD69 upregulation appears an early event in the establishment of the T_{RM} lineage.

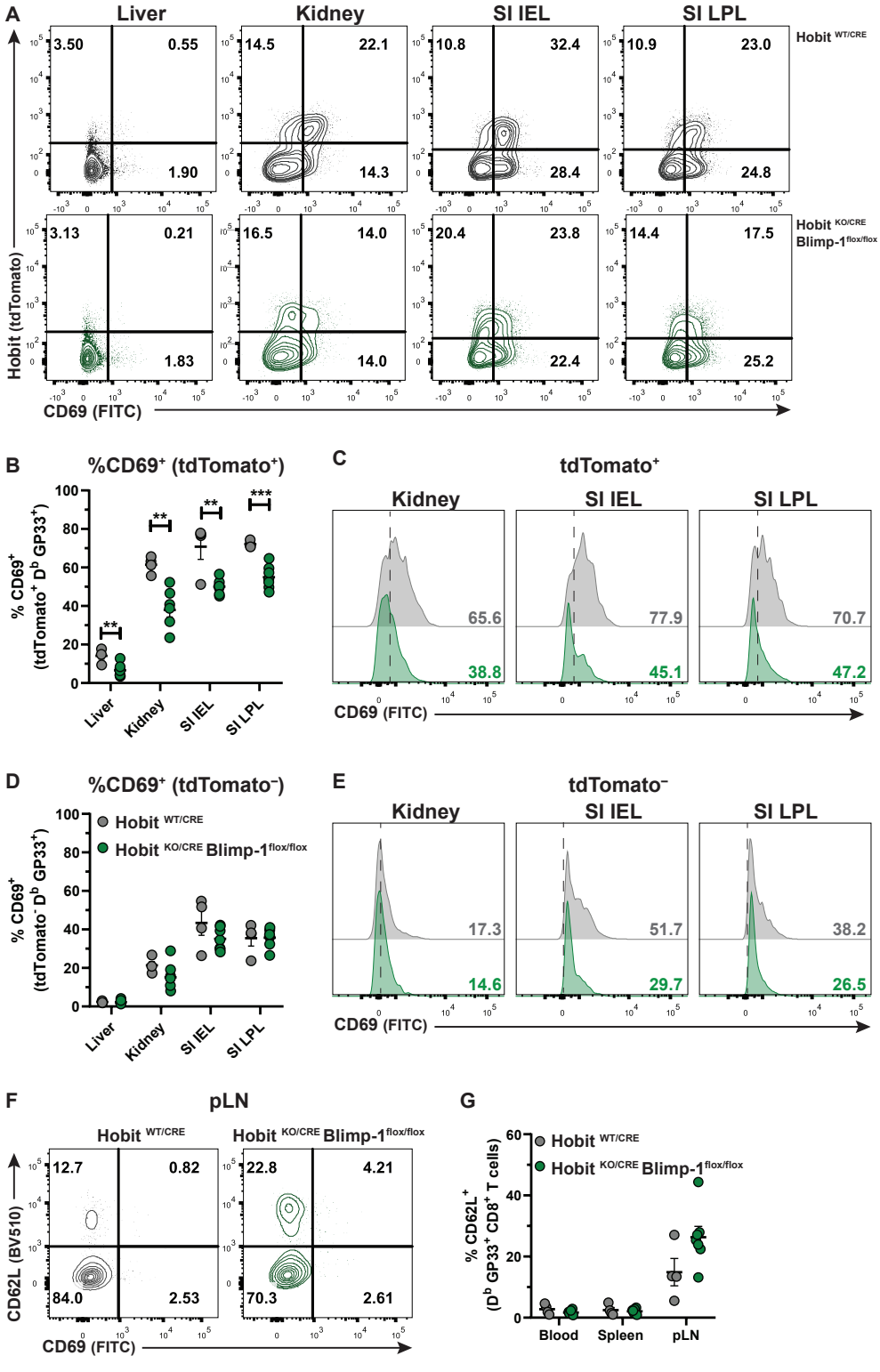
A
Liver
Kidney
SI IEL
SI LPL
Hobit WT/CRE
Hobit KO/CRE Blimp-1flox/flox
Hobit (tdTomato)
CD69 (FITC)
3.50
0.55
1.90
14.5
22.1
14.3
10.8
32.4
28.4
10.9
23.0
24.8
3.13
0.21
1.83
16.5
14.0
14.0
20.4
23.8
22.4
14.4
17.5
25.2
B
%CD69+ (tdTomato+)
% CD69+ (tdTomato+ DbGP33+)
Liver
Kidney
SI IEL
SI LPL
C
tdTomato+
Kidney
SI IEL
SI LPL
65.6
38.8
77.9
45.1
70.7
47.2
CD69 (FITC)
D
%CD69+ (tdTomato−)
Hobit WT/CRE
Hobit KO/CRE Blimp-1flox/flox
% CD69+ (tdTomato- DbGP33+)
Liver
Kidney
SI IEL
SI LPL
E
tdTomato−
Kidney
SI IEL
SI LPL
17.3
14.6
51.7
29.7
38.2
26.5
CD69 (FITC)
F
pLN
Hobit WT/CRE
Hobit KO/CRE Blimp-1flox/flox
CD62L (BV510)
12.7
0.82
84.0
2.53
22.8
4.21
70.3
2.61
CD69 (FITC)
G
Hobit WT/CRE
Hobit KO/CRE Blimp-1flox/flox
% CD62L+ (DbGP33+ CD8+ T cells)
Blood
Spleen
pLN

Figure 5. Hobit and Blimp1 promote CD69 expression on T_{RM} precursors.
(A) Representative flow cytometry plots display CD69 and tdTomato expression within Gp33^{+} CD8^{+} T cells in the indicated tissues of HR and HR^{KO} Bl^{fl} mice at day 8 after *LCMV* infection. (B-E) The percentage of CD69 expression was quantified in (B) tdTomato^{+} and (D) tdTomato^{-} virus-specific CD8^{+} T cells of HR and HR^{KO} Bl^{fl} mice. (C, E) Representative histograms display CD69 expression in (C) tdTomato^{+} and (E) tdTomato^{-} virus-specific CD8^{+} T cells in the indicated tissues of HR (grey) and HR^{KO} Bl^{fl} (green) mice. (F) Representative flow cytometry plots display CD69 and CD62L expression within Gp33^{+} CD8^{+} T cells in the pLNs of HR and HR^{KO} Bl^{fl} mice at day 8 after *LCMV* infection. (G) The percentage of CD62L expression was quantified within Gp33^{+} CD8^{+} T cells in the indicated tissues of HR and HR^{KO} Bl^{fl} mice at day 8 after *LCMV* infection. Combined data from two independent experiments (n = 4-7). Symbols represent individual mice. Error bars represent mean ± SEM. Unpaired t-test; ** $P < 0.01$, *** $P < 0.001$.

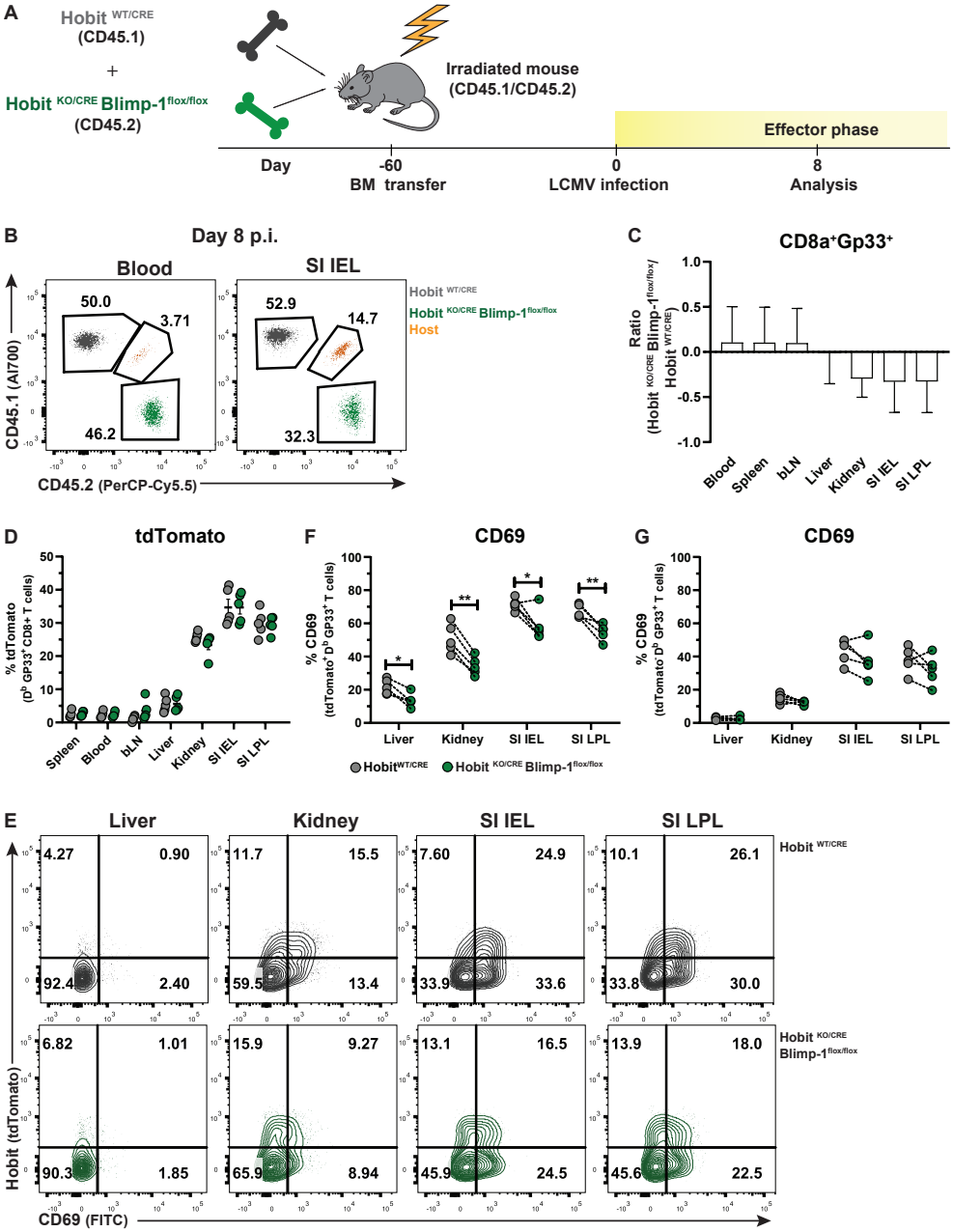

Figure 6. Hobit and Blimp1 promote CD69 expression on T_{RM} precursors.
(A) The experimental setup of *LCMV* infection in mixed bone marrow (BM) chimeras from HR and HR^{KO} BI^{fl} mice (1:1 ratio) is shown. (B) Representative flow cytometry plots display CD45.1 and CD45.2 expression to identify the contribution of HR ($CD45.1^+$) and HR^{KO} BI^{fl} fl ($CD45.2^+$) to the $Gp33^+$ $CD8^+$ T cell population of chimeric mice at day 8 p.i. (C) The log2 ratio of the percentage of $Gp33^+$ $CD8^+$ T cells of HR^{KO} BI^{fl} mice relative to those of HR mice was quantified in the indicated tissues. (D) The percentage of tdTomato expression was quantified in the HR and HR^{KO} BI^{fl} compartments of $Gp33^+$ $CD8^+$ T cells in the indicated tissues of chimeric mice. (E) Representative flow cytometry plots display tdTomato and CD69 expression within the HR and HR^{KO} BI^{fl} compartment of $Gp33^+$ $CD8^+$ T cells in the indicated tissues of chimeric mice. (F, G) The percentage of CD69 expression was quantified in (F) $tdTomato^+$ and (G) $tdTomato^-$ virus-specific $CD8^+$ T cells of the HR and HR^{KO} BI^{fl} compartment of chimeric mice. Symbols represent individual mice. Dotted lines connect paired samples. Representative data of one ($n = 5$) out of two independent experiments. Paired *t*-test; * $P < 0.05$; ** $P < 0.01$.

Discussion

The differentiation of $CD8^+$ T cells into distinct subsets of memory $CD8^+$ T cells is a tightly regulated process under the control of a network of transcription factors. Here, we studied the role of Hobit and Blimp1 during T_{RM} development using mice that allowed tracking of the T_{RM} lineage through the Hobit reporter and enabled the removal of these transcription factors from the T_{RM} lineage. We found that T_{RM} precursors could still be formed in the absence of Hobit and Blimp1, but both transcription factors were required to instruct the upregulation of the tissue-retention molecule CD69 on T_{RM} precursors. The impact of Hobit and Blimp1 on effector T cells favored T_{RM} development and suppressed T_{CM} formation during the memory phase of the immune response. These findings underline an essential role of Hobit and Blimp1 at the branching point of the T_{CM} and T_{RM} lineages, by promoting retention of T_{RM} precursors, while restricting T_{CM} formation.

We have previously shown that Hobit and Blimp1 drive T_{RM} differentiation[22], but the role of these transcription factors in early events of T_{RM} development remained unresolved due to the inability to identify T_{RM} precursors. We and others have shown that effector $CD8^+$ T cells destined to develop into T_{RM} already separate from other memory T cell lineages at early stages of the immune response[19–21]. Given that these committed T_{RM} precursors uniformly expressed Hobit, we had the opportunity to interrogate the role of Hobit and Blimp1 in early events of T_{RM} differentiation using Hobit and Blimp1 deficient Hobit reporter mice. We found that Hobit was not essential for the formation of T_{RM} precursors as identified by expression of the Hobit reporter. Moreover, Hobit and Blimp1 did not have an effect on the distribution of $Hobit^+$ effector T cells throughout peripheral organs, suggesting that these transcription factors do not instruct the trafficking of T_{RM} precursors to peripheral tissues. In contrast, we found that Hobit and Blimp1 were essential for the expression of the tissue-retention molecule CD69 on T_{RM} precursors. Other T_{RM}-associated molecules such as CD103, CD49a or CXCR6 were not affected by the lack of Hobit and Blimp1. These observations underline an early role of Hobit and Blimp1 in the maintenance of T_{RM} precursors in the peripheral tissues, given that CD69 is important for tissue retention of T_{RM}[26]. CD69 suppresses surface expression of the tissue exit receptor S1PR1, thereby locking T cells into the tissues[27,28]. Therefore, our findings suggest that Hobit and Blimp1 are responsible for the early retention of T_{RM} precursors within the tissues through the regulation of the S1PR1-driven pathway of tissue exit.

Even though T_{RM} precursors from all studied peripheral tissues had defects in CD69 expression, T_{RM} formation was mainly affected in liver and kidney compared to the intestinal compartment. We have previously shown that both Hobit and Blimp1 drive T_{RM} development in liver, kidney, skin and small intestine[22]. The mice from this previous study completely lacked Hobit and Blimp1 in the T cell lineage resulting in defects in both terminal effector differentiation and T_{RM} differentiation. A recent study has shown the presence of terminal and memory resident populations in the small intestine, identified by Blimp1 and Id3 respectively[20]. Given that our newly developed mice are only Blimp1 deficient after Hobit upregulation, it is possible that residual $CD8^+$ T cells in the small intestine represent Blimp1-expressing terminal resident populations that develop independent of Hobit. In addition, in contrast to liver and kidney, SI IEL T_{RM} express the integrin CD103, which facilitates their binding to the epithelium and allow them to rely on additional retention mechanisms besides CD69–driven suppression of S1PR1.

The classification of effector $CD8^+$ T cells into SLECs and MPECs separates terminally differentiated cells from effector T cells with potential to differentiate into memory T cells[3,4]. However, the MPEC population does not capture heterogeneity between precursors of the T_{CM}, T_{EM} and T_{RM} lineages. The transcriptional regulation of effector T cells suggests that lineage specification of memory T cells may occur at early stages of the immune response. We have previously shown that Eomes suppresses Hobit expression and limits the development of T_{RM} precursors to favor the development of the T_{CM} lineage[17]. Here, we showed that Hobit and Blimp1 specifically favored the generation of T_{RM} while restricting the formation of T_{CM}. Our results suggest that T_{RM} precursors that are unable to persist within the tissues develop into T_{CM} in circulation. We have previously demonstrated that Hobit and Blimp1 via direct binding to the TCF1 encoding *Tcf7* locus suppress the expression of TCF1[22], which is an essential transcription factor for the development of T_{CM} cells[29]. Thus, Hobit and Blimp1 may impair T_{CM} development through suppression of the T_{CM}-inducing transcription factor TCF1. Taken together, these findings suggest that Eomes, Hobit, Blimp1 and TCF1 control a branching point in effector T cell differentiation resulting in the early separation of the T_{CM} and T_{RM} lineages.

As previously observed[22], the combined action of Hobit and Blimp1 was required to regulate T_{RM} differentiation. In contrast to double deficiency of both transcription factors, single deficiency in Hobit or Blimp1 within the T_{RM} lineage did not affect the differentiation of T_{RM} and T_{RM} precursors. The synergy between Hobit and Blimp1 was not unexpected, given that these transcription factors are homologous with high similarity in the functional zinc finger domains[30,31], which are important for the recognition and binding of DNA sequences. Indeed, both Hobit and Blimp1 bind to common motifs in the DNA and share many target genes in $CD8^+$ T cells[22,31]. These similarities in DNA binding suggest that both transcription factors act in a cooperative manner to regulate the formation of T_{RM} precursors. Importantly, the shared target genes of Hobit and Blimp1 include transcription factors that regulate tissue exit such as KLF2 and TCF1 and tissue exit receptors themselves such as S1PR1 and CCR7[22]. Therefore, it is possible that the regulation of CD69 expression is downstream of the collaborative Hobit and Blimp1 driven transcriptional regulation of S1PR1 expression.

In contrast to their overlapping targets, Hobit and Blimp1 have divergent expression patterns in $CD8^+$ T cells. In comparison to Hobit, which is confined to the T_{RM} lineage, Blimp1 has a much wider expression pattern. Blimp1 is upregulated in $CD8^+$ T cells after encountering cognate antigen[32,33] and it acquires its maximum expression in terminal effector $CD8^+$ T cells to promote their terminal differentiation[8,9,20]. In contrast to these findings, we did not observe that Blimp1 impacted terminal differentiation upon establishment of the T_{RM} lineage despite expression of KLRG1 and CX3CR1 on a subset of $Hobit^+$ effector $CD8^+$ T cells[17]. These observations suggest that Blimp1 may acquire distinct roles during the process of T cell differentiation, driving terminal differentiation upon T cell priming and promoting tissue retention upon establishment of the T_{RM} lineage.

Hobit and Blimp1 are an integrated part of a larger transcriptional program governing the differentiation of effector $CD8^+$ T cells into different lineages of memory precursors and terminal effectors. Transcription factors, such as Bcl6, Id3 and Eomes, have been implicated in favoring the differentiation of memory precursors, in particular those upstream of T_{CM}[12–16]. Other transcription factors, such as Tbet, Id2, Runx3 and Notch appear to preferentially drive terminal differentiation of effector $CD8^+$ T cells as well as the development of T_{RM}[34–36]. Thus, all of these transcriptional regulators appear important to regulate distinct aspects of T_{RM} differentiation. In line with our previous findings in T_{RM}[22], we have shown that Hobit and Blimp1 have an important early role for the retention of T_{RM} precursors within the tissues through sustained suppression of tissue exit pathways and upregulation of CD69, which counteracts tissue exit. Thus, Hobit and Blimp1 appear an essential pair of transcription factors in the transcriptional network regulating the developmental pathway of T_{RM}.

Methods

Mice

Wild-type CD45.2^{+} (C57BL/6JRj) mice were purchased from Janvier, wild-type CD45.1^{+} (B6.SJL-Ptprc^{a} Pepc^{b}/BoyJ) mice were purchased from the Jackson Laboratory and both of these lines were crossed to obtain CD45.1 x CD45.2 mice. Hobit$^{tdTomato/WT}$ (HR) (B6-Tg (Zfp683-tdTomato-P2A-Cre-P2A-DTR)) mice were developed at Ozgene (Perth, Australia) as previously described[23]. Hobit$^{tdTomato/KO}$ Blimp1$^{flox/flox}$ (HR^{KO} Bl^{fl}), Hobit$^{tdTomato/KO}$ (HR^{KO}) and Hobit$^{tdTomato/WT}$ Blimp1$^{flox/flox}$ (HR Bl^{fl}) were generated by crossing HR with Hobit^{KO} and/or Blimp1$^{flox/flox}$ mice[8,30]. HR Blimp1$^{GFP/WT}$ were generated by crossing of HR and Blimp-1$^{GFP/WT}$ mice[37]. CD45.1 x CD45.2 mice were used as recipients for the generation of mixed bone marrow (BM) chimeric mice. Following irradiation (2 × 5 gray), recipient mice were reconstituted by intravenous transfer of 2 × 10^{7} BM cells. Recipients were used in experiments 8 weeks after reconstitution. Chimerism was analyzed in the blood prior to experiments using the congenic markers CD45.1 and CD45.2 to establish the relative size of host and donor compartments. All mice were maintained under specific pathogen-free (SPF) conditions in the animal facility of the Netherlands Cancer Institute (NKI). Experimental mice were age matched and between 8-12 weeks at the start of the experiment. Both female and male mice were used for this study. For bone marrow chimeras, donor and recipient mice were sex-matched. Animal experiments were conducted according to institutional and national guidelines.

LCMV infection

Mice were infected intraperitoneally with 1 × 10^{5} plaque-forming units (PFU) of *LCMV* Armstrong obtained from the European Virus Archive (EVAg). Infected mice were sacrificed and organs were collected for analysis of CD8^{+} T cell responses at the indicated time points after infection.

Tissue preparation

SI LPL and IEL preparations were obtained from the small intestine. After removal of residual fatty tissue, Peyer's patches, and feces, the small intestine was cut into pieces of 1 cm and incubated in Hanks' balanced slat solution (HBSS, Gibco) with 10% fetal calf serum (FCS), 5 mM EDTA, and 1 mM dithiothreitol (DTT) for 30 min at 37°C. After repeated vortexing, the IEL fraction was released from the tissue and isolated by filtering through a 70 µm cell strainer. Subsequently, IEL-depleted pieces of the intestine were washed in HBSS supplemented with 2% FCS and enzymatically digested for 30 min at 37 °C with 375 U/mL Collagenase Type I (Worthington) and 0.15 mg/mL DNase I (Roche, from bovine pancreas, grade II) in RPMI 1640 (supplemented with 10% FCS) to isolate the LPL fraction. Similarly, kidneys, which were cut into pieces of 1 mm^{3}, were enzymatically digested for 30 min at 37°C with 750 U/mL Collagenase Type I (Worthington) and 0.31 mg/mL DNase I (Roche, from bovine pancreas, grade II) in RPMI 1640 (supplemented with 10% FCS). Single cell suspensions from the LPL fraction of small intestine, kidney, spleen, LNs and liver were prepared by mechanical disruption via passing through a 70 µm cell strainer. The isolated

lymphocytes from liver, kidney and SI IEL and LPL were purified by density centrifugation on a 60%/40% Percoll gradient (GE Healthcare). BM was isolated from tibia and femur by crushing the bones in PBS or flushing them with PBS. Single cell suspensions of BM were obtained by passing through a 70 µm cell strainer. Contaminating erythrocytes were removed using red blood cell lysis buffer (155mM NH4Cl, 10mM KHCO3, 0,1mM EDTA).

Flow cytometry

Cells were incubated with antibodies and tetramers for 30 min at 4°C and washed with PBS (supplemented with 0.5 % (v/v) FCS) to remove unbound reagents. Antibodies were purchased from Biolegend, eBioscience, BD Biosciences, or Thermo Fisher Scientific as listed in the table below. H-2 Db KAVYNFATC (Gp33) tetramers (kindly provided by R. Arens, Leiden University Medical Center, Leiden) were used to detect virus-specific $CD8^+$ T cells after *LCMV* infection. Exclusion of dead cells was performed with the live/dead fixable near-IR dead cell stain kit (Thermo Fisher Scientific). Samples were acquired on LSR Fortessa or FACSymphony flow cytometers (BD Biosciences), and data was analyzed using FlowJo V10 software (Tree Star). Cell sorting was performed using an Aria III (BD Biosciences).

Antibody	Clone	Supplier	Productnr.
CD103	2E7	Biolegend	121408
CD103	M290	BD Biosciences	557495
CD127	A7R34	Biolegend	135027
CD3	17A2	eBioscience	56-0032-82
CD4	GK1.5	eBioscience	11-0041-85
CD4	RM4-5	ThermoFisher Scientific	Q10092
CD44	IM7	BD Biosciences	564392
CD44	IM7	Biolegend	103030
CD45.1	A20	Biolegend	110714, 110706
CD45.2	104	eBioscience	56-0454
CD62L	MEL-14	Biolegend	104441
CD69	H1.2F3	BD Biosciences	564684
CD69	H1.2F3	Biolegend	104506
CD69	H1.2F3	eBioscience	25-0691
$CD8^+\alpha$	53-6.7	BD Biosciences	563786
$CD8^+\alpha$	53-6.7	Biolegend	100734
$CD8^+\alpha$	53-6.7	eBioscience	56-0081-82
KLRG1	2F1	BD Biosciences	740279
KLRG1	2F1	Biolegend	138416
TCRβ	H57-597	Biolegend	109224

DNA isolation

Memory CD8$^+$ T cell populations were FACS-sorted from the liver and SI IEL of *LCMV*-infected Hobit$^{tdTomato/WT}$ and Hobit$^{tdTomato/KO}$Blimp$^{fl/fl}$ mice based on TCRβ$^+$ CD8$^+$ expression and separated into Hobit$^+$ and Hobit$^-$ fractions using tdTomato expression. Control naïve CD8$^+$ T cells (CD44$^-$CD62L$^+$) were isolated from the spleen of Hobit$^{tdTomato/WT}$ mice. Sorted cells were lysed overnight in lysis buffer (100 mM Tris-HCl; 5 mM EDTA pH 8.0; 0.2 % SDS; 200 mM NaCl, 200 µg/mL Proteinase K) at 56°C in a rotator set at 400 rpm. The lysates were centrifuged (13000 rpm, 30 min, RT) and the supernatants were mixed with an equal volume of isopropanol to precipitate the genomic DNA. After centrifugation (13000 rpm, 15 min, RT) the DNA pellet was washed in 70% (v/v) ethanol (13.000 rpm, 15 min, RT). After air-drying the DNA pellet was dissolved in ddH2O (37°C, 400 rpm, ≥ 30 min) for analysis by PCR.

PCR analysis

A double set of primers, Blimp1 deleted (Blimp1^{DEL}) and Blimp non-deleted (Blimp1ND), were used to assess the efficiency of the Hobit-driven Cre-recombinase to delete Blimp1 (table S2)[8]. The expected amplicon sizes of the PCR for Blimp1^{DEL} and Blimp1ND are provided in the table below. The amplified material was loaded on a 2% agarose gel, separated by gel electrophoresis (100V, Mupid-One, BioRad Sub-Cell GT) and imaged using the InGenius LHR Gel Imagining System (Syngene) to examine Cre-recombinase driven deletion of the Blimp1 locus.

Gene	Primer	Sequence	Amplicon size (bp).
Blimp1ND	Floxed non deleted Fw	GGCAAGATCAAGTATGAGTGC	765
Blimp1ND	Floxed common Rv	TGAGTAGTCACAGAGTACCCA	
Blimp1^{DEL}	Floxed deleted Fw	AGGTGTCTAGCCTTTGTATTTG	611
Blimp1^{DEL}	Floxed common Rv	TGAGTAGTCACAGAGTACCCA	

RNA-seq analysis

Previously published and normalized RNA-seq data of sorted murine CD8$^+$ T cell subsets after *LCMV* infection[17] and after *Listeria monocytogenes* OVA[23] was analyzed for the expression of *Prdm1* (encoding Blimp1) at day 8 p.i and day >30, respectively.

Statistical analysis

Statistical analysis was performed using Prism 8 (GraphPad). Statistical significance was calculated using the unpaired Student's *t*-test for groups that were normally distributed, and using the Mann-Whitney U test for groups that were not normally distributed. For paired samples, paired two-tailed Student's t test was employed. For comparison of more than two groups, one-way ANOVA was used. Unless otherwise indicated, differences were not statistically significant. *P*-values of <0.05 were considered statistically significant (* $P < 0.05$; ** $P < 0.01$; *** $P < 0.001$; **** $P < 0.0001$).

Author contributions

L.P.V., R.L.R.E.T., A.B.C., H.A., R.A.W.v.L., R.S. and K.P.J.M.v.G. designed the experiments. L.P.V., R.L.R.E.T., A.B.C, H.A., N.A.M.K., A.A.B. and F.M.B. performed the experiments. L.P.V., R.L.R.E.T., A.B.C., and H.A. analyzed the data. L.P.V. and K.P.J.M.v.G. wrote the manuscript. All of the authors critically revised the manuscript for important intellectual content.

Conflicts of interest

The authors declare no financial or commercial conflict of interest.

Data availability statement

The data that support the findings of this study are available from the corresponding author upon reasonable request.

Acknowledgements

We would like to thank the members of the van Gisbergen laboratory and the Department of Hematopoiesis for fruitful discussions. We thank Dr. Ramon Arens (Leiden University Medical Center) for providing *LCMV* Db Gp33 tetramers. L.P.V. and K.P.J.M.v.G. were supported by Vidi grant 917.13.338 from NWO and a fellowship of the Landsteiner Foundation of Blood Transfusion Research. R.S. was supported by a Fellowship from the Alexander von Humboldt Foundation and by Veni grant 016.186.116 from the Netherlands Organization for Scientific Research (NWO).

References

1 Butz EA, Bevan MJ. Massive expansion of antigen-specific CD8+ T cells during an acute virus infection. Immunity 1998; 8: 167–75.
2 Williams MA, Bevan MJ. Effector and Memory CTL Differentiation. Annu Rev Immunol 2007; 25: 171–192.
3 Joshi NS, Cui W, Chandele A, Lee HK, Urso DR, Hagman J et al. Inflammation directs memory precursor and short-lived effector CD8+(+) T cell fates via the graded expression of T-bet transcription factor. Immunity 2007; 27: 281–295.
4 Kaech SM, Tan JT, Wherry EJ, Konieczny BT, Surh CD, Ahmed R. Selective expression of the interleukin 7 receptor identifies effector CD8+ T cells that give rise to long-lived memory cells. Nat Immunol 2003; 4: 1191–8.
5 Sallusto F, Lenig D, Förster R, Lipp M, Lanzavecchia A. Two subsets of memory T lymphocytes with distinct homing potentials and effector functions. Nature 1999; 401: 708–712.
6 Gebhardt T, Wakim *Lm*, Eidsmo L, Reading PC, Heath WR, Carbone FR. Memory T cells in nonlymphoid tissue that provide enhanced local immunity during infection with herpes simplex virus. Nat Immunol 2009; 10: 524–530.
7 Schenkel JM, Fraser KA, Vezys V, Masopust D. Sensing and alarm function of resident memory CD8+ T cells. Nat Immunol 2013; 14: 509–513.
8 Kallies A, Xin A, Belz GT, Nutt SL. Blimp-1 Transcription Factor Is Required for the Differentiation of Effector CD8+ T Cells and Memory Responses. Immunity 2009; 31: 283–295.
9 Rutishauser RL, Martins GA, Kalachikov S, Chandele A, Parish IA, Meffre E et al. Transcriptional Repressor Blimp-1 Promotes CD8+ T Cell Terminal Differentiation and Represses the Acquisition of Central Memory T Cell Properties. Immunity 2009; 31: 296–308.
10 Backer RA, Helbig C, Gentek R, Kent A, Laidlaw BJ, Dominguez CX et al. A central role for Notch in effector CD8+ T cell differentiation. Nat Immunol 2014; 15: 1143–1151.
11 Cruz-Guilloty F, Pipkin ME, Djuretic IM, Levanon D, Lotem J, Lichtenheld MG et al. Runx3 and T-box proteins cooperate to establish the transcriptional program of effector CTLs. J Exp Med 2009; 206: 51–59.
12 Yang CY, Best JA, Knell J, Yang E, Sheridan AD, Jesionek AK et al. The transcriptional regulators Id2 and Id3 control the formation of distinct memory CD8+ T cell subsets. Nat Immunol 2011; 12: 1221–9.
13 Banerjee A, Gordon SM, Intlekofer AM, Paley MA, Mooney EC, Lindsten T et al. Cutting edge: The transcription factor eomesodermin enables CD8+ T cells to compete for the memory cell niche. J Immunol 2010; 185: 4988–92.
14 Intlekofer AM, Takemoto N, Wherry EJ, Longworth SA, Northrup JT, Palanivel VR et al. Effector and memory CD8+ T cell fate coupled by T-bet and eomesodermin. Nat Immunol 2005; 6: 1236–1244.
15 Ichii H, Sakamoto A, Kuroda Y, Tokuhisa T. Bcl6 acts as an amplifier for the generation and proliferative capacity of central memory CD8+ T cells. J Immunol 2004; 173: 883–91.
16 Ji Y, Pos Z, Rao M, Klebanoff CA, Yu Z, Sukumar M et al. Repression of the DNA-binding inhibitor Id3 by Blimp-1 limits the formation of memory CD8+ T cells. Nat Immunol 2011; 12: 1230–7.
17 Parga-Vidal L, Behr FM, Kragten NAM, Nota B, Wesselink TH, Kavazović I et al. Hobit identifies tissue-resident memory T cell precursors that are regulated by Eomes. Sci Immunol 2021; 6. doi:10.1126/sciimmunol.abg3533.
18 Iborra S, Martínez-López M, Khouili SC, Enamorado M, Cueto FJ, Conde-Garrosa R et al. Optimal Generation of Tissue-Resident but Not Circulating Memory T Cells during Viral Infection Requires Crosspriming by DNGR-1+ Dendritic Cells. Immunity 2016; 45: 847–860.
19 Kok L, Dijkgraaf FE, Urbanus J, Bresser K, Vredevoogd DW, Cardoso RF et al. A committed tissue-resident memory T cell precursor within the circulating CD8+ effector T cell pool. J Exp Med 2020; 217. doi:10.1084/jem.20191711.
20 Milner JJ, Toma C, He Z, Kurd NS, Nguyen QP, McDonald B et al. Heterogenous Populations of Tissue-Resident CD8+ T Cells Are Generated in Response to Infection and Malignancy. Immunity 2020; 52: 808-824.e7.
21 Kurd NS, He Z, Louis TL, Milner JJ, Omilusik KD, Jin W et al. Early precursors and molecular determinants of tissue-resident memory CD8+ T lymphocytes revealed by single-cell RNA sequencing. Sci Immunol 2020; 5. doi:10.1126/sciimmunol.aaz6894.
22 Mackay LK, Minnich M, Kragten NAMM, Liao Y, Nota B, Seillet C et al. Hobit and Blimp1 instruct a universal transcriptional program of tissue residency in lymphocytes. Science (80-) 2016; 352: 459–463.
23 Behr FM, Parga-Vidal L, Kragten NAM, van Dam TJP, Wesselink TH, Sheridan BS et al. Tissue-resident memory CD8+ T cells shape local and systemic secondary T cell responses. Nat Immunol 2020; 21: 1070–1081.

24 Kragten NAM, Behr FM, Vieira Braga FA, Remmerswaal EBM, Wesselink TH, Oja AE et al. Blimp-1 induces and Hobit maintains the cytotoxic mediator granzyme B in $CD8^+$ T cells. Eur J Immunol 2018; 48: 1644–1662.

25 Shin H, Blackburn SD, Intlekofer AM, Kao C, Angelosanto JM, Reiner SL et al. A Role for the Transcriptional Repressor Blimp-1 in $CD8^+$ T Cell Exhaustion during Chronic Viral Infection. Immunity 2009; 31: 309–320.

26 Mackay LK, Rahimpour A, Ma JZ, Collins N, Stock AT, Hafon M-L et al. The developmental pathway for CD103+$CD8^+$ tissue-resident memory T cells of skin. Nat Immunol 2013; 14: 1294–1301.

27 Matloubian M, Lo CG, Cinamon G, Lesneski MJ, Xu Y, Brinkmann V et al. Lymphocyte egress from thymus and peripheral lymphoid organs is dependent on S1P receptor 1. Nature 2004; 427: 355–360.

28 Shiow LR, Rosen DB, Brdicková N, Xu Y, An J, Lanier LL et al. CD69 acts downstream of interferon-alpha/beta to inhibit S1P1 and lymphocyte egress from lymphoid organs. Nature 2006; 440: 540–4.

29 Zhou X, Yu S, Zhao DM, Harty JT, Badovinac VP, Xue HH. Differentiation and Persistence of Memory $CD8^+$ T Cells Depend on T Cell Factor 1. Immunity 2010; 33: 229–240.

30 van Gisbergen KPJM, Kragten NAM, Hertoghs KML, Wensveen FM, Jonjic S, Hamann J et al. Mouse Hobit is a homolog of the transcriptional repressor Blimp-1 that regulates NKT cell effector differentiation. Nat Immunol 2012; 13: 864–871.

31 Vieira Braga FA, Hertoghs KML, Kragten NAM, Doody GM, Barnes NA, Remmerswaal EBM et al. Blimp-1 homolog Hobit identifies effector-type lymphocytes in humans. Eur J Immunol 2015; 45: 2945–2958.

32 Martins GA, Cimmino L, Shapiro-Shelef M, Szabolcs M, Herron A, Magnusdottir E et al. Transcriptional repressor Blimp-1 regulates T cell homeostasis and function. Nat Immunol 2006; 7: 457–65.

33 Kallies A, Hawkins ED, Belz GT, Metcalf D, Hommel M, Corcoran *Lm* et al. Transcriptional repressor Blimp-1 is essential for T cell homeostasis and self-tolerance. Nat Immunol 2006; 7: 466–74.

34 Mackay LK, Wynne-Jones E, Freestone D, Pellicci DG, Mielke LA, Newman DM et al. T-box Transcription Factors Combine with the Cytokines TGF-β and IL-15 to Control Tissue-Resident Memory T Cell Fate. Immunity 2015; 43: 1101–1111.

35 Milner JJ, Toma C, Yu B, Zhang K, Omilusik K, Phan AT et al. Runx3 programs $CD8^+$ T cell residency in non-lymphoid tissues and tumours. Nature 2017; 552: 253–257.

36 Hombrink P, Helbig C, Backer RA, Piet B, Oja AE, Stark R et al. Programs for the persistence, vigilance and control of human $CD8^+$ lung-resident memory T cells. Nat Immunol 2016; 17: 1467–1478.

37 Kallies A, Hasbold J, Tarlinton DM, Dietrich W, Corcoran lm, Hodgkin PD et al. Plasma cell ontogeny defined by quantitative changes in blimp-1 expression. J Exp Med 2004; 200: 967–77.

Supporting Information

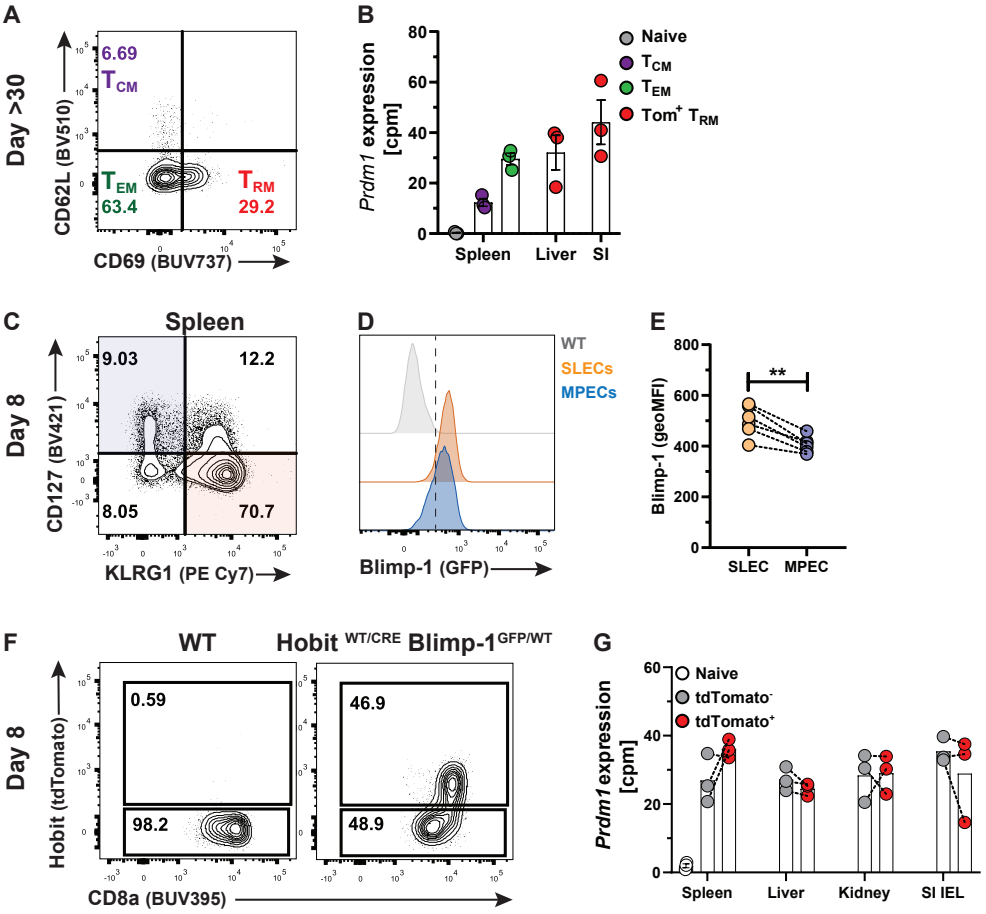

Figure S1. Hobit is restricted to the T_{RM} lineage and Blimp1 is widely expressed in antigen-experienced CD8$^+$ T cells. (A) Representative flow cytometry plot shows CD62L and CD69 expression which identifies T_{CM} (CD62L$^+$ CD69$^-$), T_{EM} (CD62L$^-$CD69$^-$) and T_{RM} (CD62L$^-$ CD69$^+$) cells, as indicated. (B) Expression (cpm) of *Prdm1* encoding Blimp1 was determined in naïve and *Listeria*-OVA-specific memory CD8$^+$ T cells by RNA sequencing. (C) Representative flow cytometry plot shows KLRG1 and CD127 expression to identify SLECs (KLRG1$^+$ CD127$^-$) and MPECs (KLRG$^-$CD127$^+$) in the spleen of HR BI^{GFP} mice. (D) Representative histogram shows expression of Blimp-1 (GFP) in the indicated cell subsets. (E) The geo MFI of GFP expression was quantified in SLECs and MPECs. (F) Representative flow cytometry plot displays the gating of tdTomato$^+$ and tdTomato$^-$ virus-specific CD8$^+$ T cells at day 8 after *LCMV* infection. (G) Expression (cpm) of Prdm1 in naïve and tdTomato$^+$ and tdTomato$^-$ *LCMV*-specific effector CD8$^+$ T cells isolated at day 8 p.i. was determined by RNA sequencing. Symbols represent individual mice. Error bars represent mean ± SEM. Dotted lines connect paired samples. (A) Representative data of one (n = 4) out of two independent experiments. (B, G) Data from one experiment (n = 3 pooled samples). (C-F) Combined data from two independent experiments (n = 6). Paired t-test; ** $P < 0.01$.

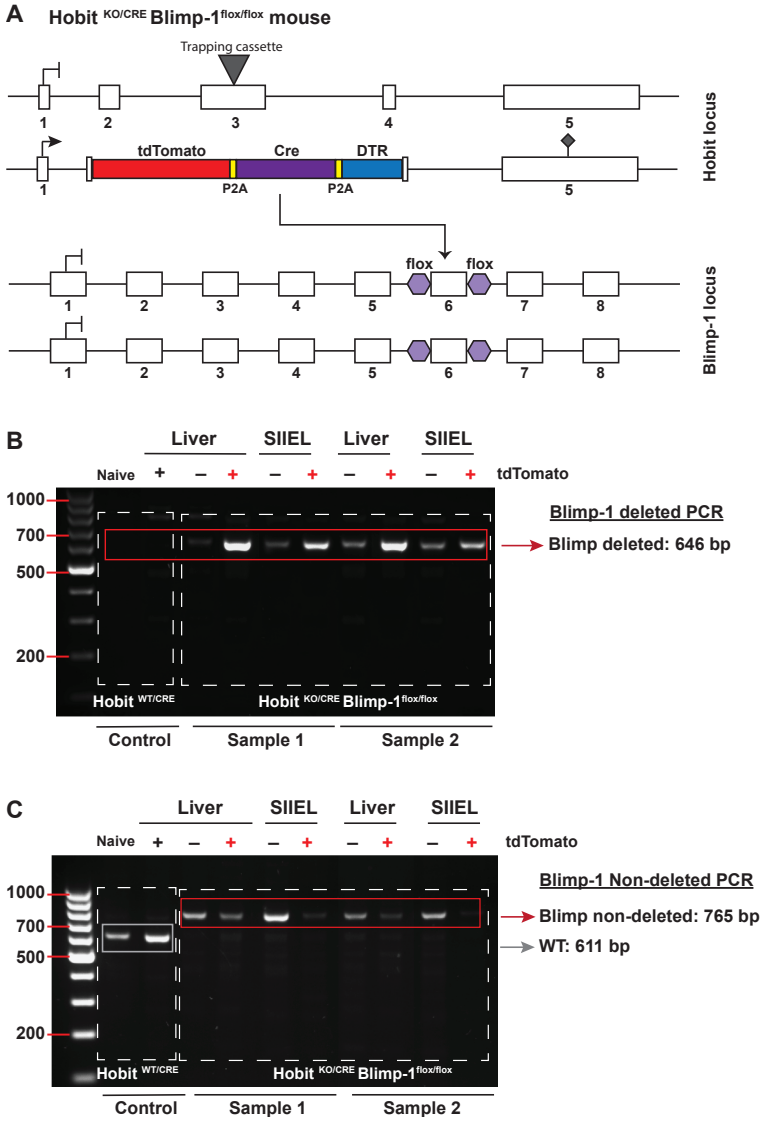

Figure S2. Blimp1 is efficiently deleted in Hobit^{+} CD8^{+} T cells of HR^{KO} Bl^{fl} mice.
(A) Schematic representation of the HR^{KO} Bl^{fl} mouse is shown. (B, C) The presence of (B) deleted Blimp1 and (C) non-deleted Blimp1 was analyzed by semi-quantitative PCR in CD8^{+} T cells isolated from the liver and SI IEL of HR^{KO} Bl^{fl} and control HR^{WT} mice at day >30 after *LCMV* infection. Data display 2 individual samples from two independent experiments.

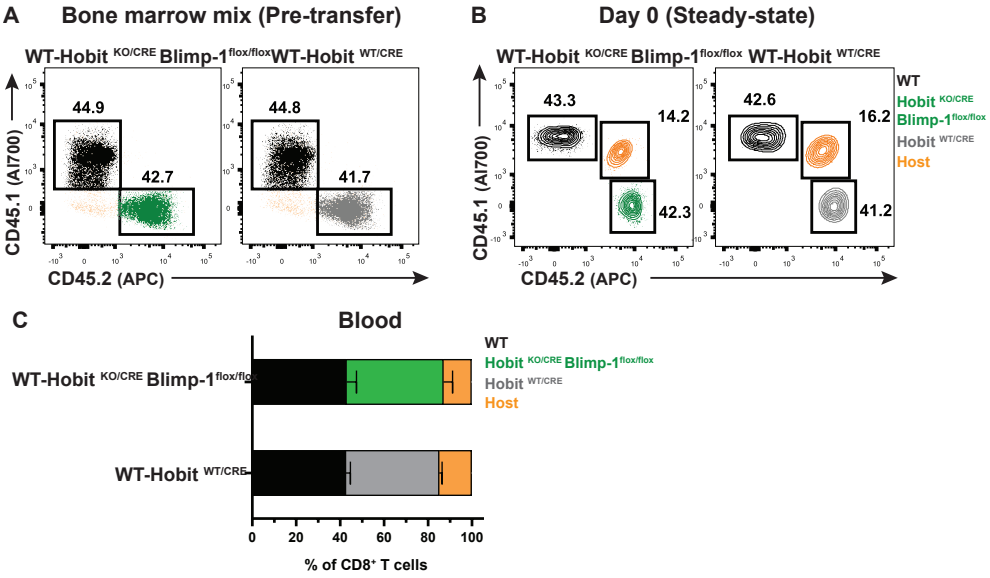

Figure S3. Contribution of different cell compartments in mixed bone marrow (BM) chimeras.
(A, B) Representative flow cytometry plots display CD45.1 and CD45.2 to identify the contribution of WT (CD45.1$^+$) and HR (CD45.2$^+$) or HR^{KO} Bl^{fl} (CD45.2$^+$) to the (A) pre-transfer BM cell mix and (B) to the total CD8$^+$ T cell fraction in the blood of chimeric mice 60 days after reconstitution and just prior to infection with *LCMV*. (C) The contribution of WT and transgenic CD8$^+$ T cells to the total CD8$^+$ T cell fraction was quantified. Representative data of one (n = 3-4) out of two independent experiments.

Figure S4. Hobit$^+$ effector CD8$^+$ T cells are enriched for an MPEC phenotype.

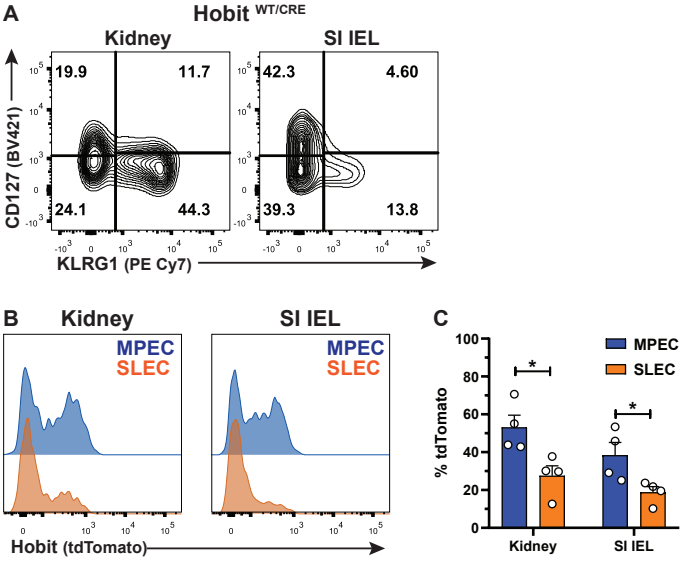

(A) Representative flow cytometry plots show expression of CD127 and KLRG1 within Gp33$^+$ CD8$^+$ T cells in the indicated tissues of HR mice. (B) Representative histograms display the expression of tdTomato within MPECs (KLRG1$^-$CD127$^+$) and SLECs (KLRG1$^+$ CD127$^-$). (C) The percentage of tdTomato expression was quantified in MPECs and SLECs in the indicated tissues. Combined data from two independent experiments (n = 4). Unpaired t-test; * P <0.05.

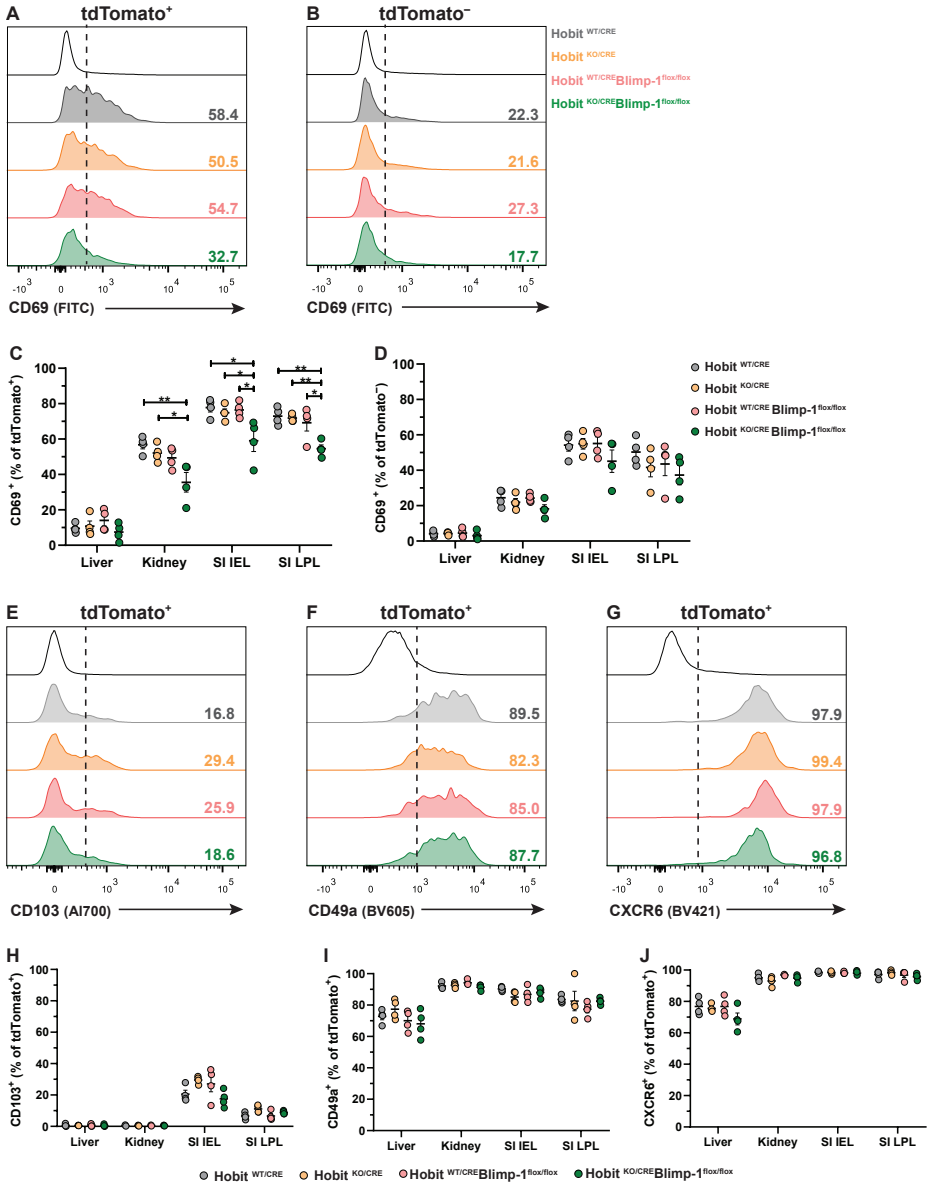

Figure S5. Hobit and Blimp1 cooperatively instruct upregulation of CD69 on T_{RM} precursors.
(A, B) Representative histograms display CD69 expression in (A) tdTomato$^+$ and (B) tdTomato$^-$ virus-specific CD8$^+$ T cells isolated from the kidney of HR, HR^{KO}, HR Bl^{fl} and HR^{KO} Bl^{fl} mice at day 8 after *LCMV* infection. (C, D) The percentage of CD69 expression was quantified in (C) tdTomato$^+$ and (D) tdTomato$^-$ virus-specific CD8$^+$ T cells. (E-G) Representative histograms display expression of (E) CD103, (F) CD49a and (G) CXCR6 on tdTomato$^+$ virus-specific CD8$^+$ T cells isolated from the SI IEL of HR, HR^{KO}, HR Bl^{fl} and HR^{KO} Bl^{fl} mice at day 8 p.i. Control sample gated on CD62L$^+$ T cells from the spleen. (H-J) The percentage of (H) CD103, (I) CD49a and (J) CXCR6 expression was quantified in tdTomato$^+$ virus-specific CD8$^+$ T cells of HR, HR^{KO}, HR Bl^{fl} and HR^{KO} Bl^{fl} mice. Symbols represent individual mice. Error bars represent mean ± SEM. (A-J) Combined data from two independent experiments (n = 4). One-way ANOVA; * $P < 0.05$; ** $P < 0.01$.

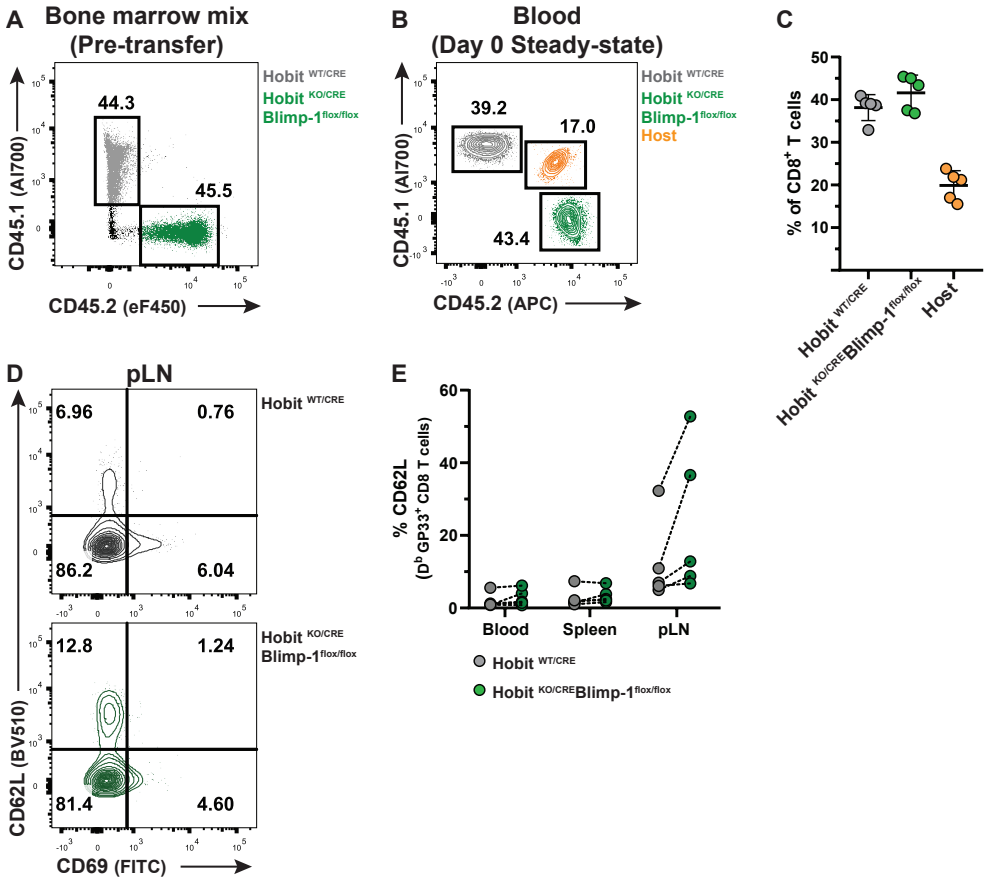

Figure S6. Hobit and Blimp1 promote CD69 expression on T_{RM} precursors in mixed bone marrow (BM) chimeras. Representative flow cytometry plots display CD45.1 and CD45.2 expression to identify the contribution of HR (CD45.1$^+$) and HR^{KO} Bl^{fl} (CD45.2$^+$) to the (A) pre-transfer BM cell mix and (B) to the total CD8$^+$ T cell fraction in the blood of chimeric mice 60 days after reconstitution and just prior to infection with *LCMV*. (C) The percentage of CD8$^+$ T cells originating from the host, and the donor HR and HR^{KO} Bl^{fl} compartments was determined. (D) Representative flow cytometry plots display CD62L and CD69 expression in Gp33$^+$ CD8$^+$ T cells from the HR and HR^{KO} Bl^{fl} compartment at day 8 p.i. with *LCMV*. (E) The percentage of CD62L expression was quantified in the HR and HR^{KO} Bl^{fl} compartment of Gp33$^+$ CD8$^+$ T cells in the indicated tissues of the chimeric mice. Symbols represent individual mice. Representative data of one ($n = 5$) out of two independent experiments. (C) Error bars represent mean ± SEM. (E) Dotted lines connect paired samples.